

Monte Carlo study of one-hole band structure in the t - J model

T. Barnes

*Physics Division and Center for Computationally Intensive Physics,
Oak Ridge National Laboratory, Oak Ridge, Tennessee 37831-6373;
and Department of Physics, University of Tennessee, Knoxville, Tennessee 37996-1200*

M. D. Kovarik

*Physics Division and Center for Computationally Intensive Physics,
Oak Ridge National Laboratory, Oak Ridge, Tennessee 37831-6373;
Department of Physics, University of Tennessee, Knoxville, Tennessee 37996-1200;
and University of Tennessee Computing Center, Knoxville, Tennessee 37996-0520*

(Received 24 April 1992)

We present Monte Carlo results for the band structure of the lowest-lying $S_{\text{tot}} = \frac{1}{2}$ one-hole band in the t - J model on 4×4 and 6×6 lattices. In this paper we report measurements for all \mathbf{k} states in the small t/J regime $0 \leq t/J \leq 0.2$, and extrapolate to $0 \leq t/J \leq 0.5$. Our results support the conjecture that the linear- t component of the bandwidth at small t/J vanishes as κ/L^2 in the bulk limit, as was anticipated on theoretical grounds; this implies that the propagation of isolated holes is strongly hindered by the staggered magnetization of the ground state. For this initial study we used a very simple trial wave function for importance sampling; it should be possible to obtain comparably accurate Monte Carlo results for band structure at appreciably larger t/J with improved importance sampling.

I. INTRODUCTION

The t - J model,¹ which is the two-dimensional Heisenberg antiferromagnet on a square lattice with a hopping term, has attracted considerable interest as a candidate model of high-temperature superconductivity. This model, defined by the Hamiltonian

$$H = -t \sum_{\langle ij \rangle, \sigma} (c_{i\sigma}^\dagger c_{j\sigma} + \text{H.c.}) + J \sum_{\langle ij \rangle} (\mathbf{S}_i \cdot \mathbf{S}_j - \frac{1}{4} n_i n_j), \quad (1)$$

incorporates the large antiferromagnetic interaction present in the copper-oxygen planes and allows hole hopping if vacancies are present. Since the high- T_c materials become superconductors with moderate hole doping away from half-filling, the t - J model should also exhibit this behavior if it incorporates the relevant dynamics and interactions.

There have been suggestions in the literature that the model may be unphysical, as hole condensation may not stop with pairs but instead may lead to phase separation.^{2,3} This apparently does occur for sufficiently small t/J , but the phase diagram of the t - J model for larger t/J is problematical. Recently this suggestion of hole phase separation for all t/J has been disputed. Evidence for a transition from the separated phase at moderate t/J , derived from high-temperature expansions, has been presented by Putikka, Luchini, and Rice.⁴ The estimated phase boundary is at $t/J \approx 0.8$ near half-filling, which decreases to $t/J \approx 0.3$ as the filling fraction approaches zero. Additional evidence against phase separation at moderate t/J has come from studies of the Hubbard model by Moreo, Scalapino, and Dagotto⁵ and Dagotto *et al.*⁶ These references find no evidence for

phase separation in the two-dimensional Hubbard model at moderately large U/t , and conclude that the t - J model probably does not phase separate for $t/J \gtrsim 1$. As the high-temperature superconductor parameter values are $t \sim 0.5$ eV and $J \approx 0.125$ eV, so that $t/J \sim 3$, the t - J model with CuO_2 parameters may give a more realistic description of the superconductors than was indicated by previous suggestions of phase separation.

Although numerical studies of the t - J model on large lattices could in principle establish the phase diagram, it has unfortunately proven difficult to study the t - J model on large lattices using numerical techniques. The large Hilbert space has restricted Lanczos investigations to at most 18 (Refs. 7 and 8) or 20 (Ref. 9) sites, and the majority of Lanczos studies have specialized to the relatively small 4×4 lattice.¹⁰⁻¹⁸

Studies of the static-hole limit on larger lattices have been reported using spin-wave theory¹⁹ and Monte Carlo techniques.^{20,21} Comparison of these results with the 4×4 case suggest that the Lanczos results may incorporate important lattice artifacts, such as degeneracies due to the hypercubical symmetry of the 4×4 lattice and large finite-size effects.

Monte Carlo studies of the t - J model are complicated by the "minus-sign problem" encountered in multi-fermion systems in more than one space dimension. (For a general discussion see the paper of Loh *et al.*²²) This problem arises from the fact that off-diagonal matrix elements of the type

$$\langle n' | (I - H_I h_r) | n \rangle \quad (2)$$

can have either sign in these systems. These matrix elements are encountered for example in evolving an initial distribution of configurations to a ground-state distribution using the operator

$$e^{-H\tau} = \lim_{\substack{h_\tau \rightarrow 0 \\ n_\tau h_\tau = \tau}} \sum_{\{n\}} |n_\tau\rangle \langle n_\tau| (I - H h_\tau) |n_{\tau-1}\rangle \langle n_{\tau-1}| \cdots |n_1\rangle \langle n_1| (I - H h_\tau) |n_0\rangle \langle n_0| \quad (3)$$

or in evaluating the partition function, which is the trace of this operator. The phases of these matrix elements may be assigned to weight factors associated with configurations generated by the algorithm, and these weights evidently can have either sign depending on the path $\mathcal{S}(\tau)$ the configuration follows in Hilbert space. The weights are then used in averages in the calculation of matrix elements, which will have considerably larger statistical errors if weights occur with both signs in comparable numbers. In measuring dispersion relations using Monte Carlo techniques one encounters a related difficulty, which is that the matrix elements [Eq. (2)] between momentum eigenstates are in general complex, and so the “minus-sign problem” generalizes to a “complex phase problem.” Despite these difficulties, recent Monte Carlo studies have found it possible to extract useful results for several systems which have minus-sign problems. These include the energy of the one-hole ground state in the t - J model²³ (which requires negative weights) and the dispersion relation of the spin-1 Heisenberg chain²⁴ (which requires complex weights).

In this paper we show that the problem of determining t - J model dispersion relations using a Monte Carlo technique can be solved formally using complex weights. Although cancellations between weights do lead to a considerable increase in the statistical noise relative to Heisenberg model simulations in practice, one may nonetheless obtain interesting results for one-hole band structure using currently available computing facilities.

II. METHOD

For our simulations we employ the “guided random walk” (GRW) algorithm, which was introduced by Barnes, Daniell, and Storey²⁵ as a method for Hamiltonian lattice gauge theory, and has since been generalized to discrete degrees of freedom^{26,27}; applications include U(1) lattice gauge theory,²⁸ multi-quark systems in the nonrelativistic quark model,²⁹ the Heisenberg antiferromagnet,^{20,26,27,30,31} and the t - J_z model.³² The GRW algorithm is unlike GFMC in that it does not use a fluctuating population of “walkers,” but instead generates a single unbranched random walk and associates a path-dependent weight factor with that walk. The weights of many such walks are then used in averages to determine energies, as we shall discuss. The weights can also be used in a straightforward manner to give unbiased $|\psi_0|^2$ -weighted ground-state matrix elements,³³ which is a difficult problem for some algorithms. (See Barnes³³ and Manousakis³⁴ for reviews of this and other algorithms used in studies of the Heisenberg model.)

In the GRW algorithm one generates a random walk in Hilbert space, in which the path followed by the configuration is parametrized by the Euclidean time τ . One begins the random walk at $\tau = 0$ with a chosen initial configuration [which in our case is a hole at (0,0) in a Néel state], and increments the Euclidean time in steps

of h_τ . After each time step the walk has the option of making a transition from the current configuration $\mathcal{S}(\tau)$ to a new configuration $\mathcal{S}'(\tau)$ with probability

$$P(\mathcal{S} \rightarrow \mathcal{S}') = r_{\mathcal{S}\mathcal{S}'} h_\tau, \quad (4)$$

where the stepping-rate matrix $r_{\mathcal{S}\mathcal{S}'}$ is

$$r_{\mathcal{S}\mathcal{S}'} = \left| -\langle \mathcal{S}' | H_I | \mathcal{S} \rangle \frac{\Psi_0^g(\mathcal{S}')}{\Psi_0^g(\mathcal{S})} \right|; \quad (5)$$

after the $\mathcal{S} \rightarrow \mathcal{S}'$ transition is attempted, the Euclidean time is incremented to $\tau + h_\tau$, and the process is repeated. In these formulas H_I is the off-diagonal part of the Hamiltonian, H_0 is the diagonal part (here the “Ising energy” $J \sum_{\langle ij \rangle} (S_i^z S_j^z - n_i n_j / 4)$, and $\Psi_0^g(\mathcal{S})$ is an approximate ground-state wave function which is used by the algorithm for importance sampling; the definition of $r_{\mathcal{S}\mathcal{S}'}$ [Eq. (5)] implies that the walks preferentially explore regions where $|\Psi_0^g|$ is large. One calculates a weight factor associated with each walk, which is

$$w(\tau_1) = \exp(i\phi) \exp \left\{ -\int_0^{\tau_1} \left(H_0(\mathcal{S}(\tau)) - \sum_{\mathcal{S}'} r_{\mathcal{S}\mathcal{S}'} \right) d\tau \right\}. \quad (6)$$

This weight factor is a function of the path $\mathcal{S}(\tau)$ followed by the walk, and in general has an overall phase $\exp(i\phi)$. When averaged over random walks the weight asymptotically approaches an exponential in the ground-state energy,

$$\lim_{\tau \rightarrow \infty} \langle w(\tau) \rangle = c \exp(-E_0 \tau). \quad (7)$$

One may therefore determine energies from the average weight at two Euclidean times,

$$E_0^{\text{estm}} = \lim_{\tau_1, \tau_2 \rightarrow \infty} \ln \left(\langle w(\tau_1) \rangle / \langle w(\tau_2) \rangle \right) / (\tau_2 - \tau_1). \quad (8)$$

In practice there are biases due to the use of a finite sample of walks, a finite Euclidean step size h_τ , and finite measurement times τ_1 and τ_2 , and one must be careful to establish that these systematic errors are within required limits.

The weight phase $\exp(i\phi)$ is the phase of the product of $(-H_I)$ matrix elements encountered in all transitions executed by the walk:

$$\exp(i\phi) = \prod_{\substack{\mathcal{S} \rightarrow \mathcal{S}' \\ \text{transitions}}} \frac{-\langle \mathcal{S}' | H_I | \mathcal{S} \rangle}{\left| -\langle \mathcal{S}' | H_I | \mathcal{S} \rangle \right|}. \quad (9)$$

In problems such as the determination of the ground-state energy of the Heisenberg antiferromagnet we minimize statistical errors by choosing our basis $\{|\mathcal{S}\rangle\}$ so this phase is always +1, which requires that all nonzero off-diagonal Hamiltonian matrix elements be negative. In the t - J model with a \hat{z} -diagonal spin basis this is not

possible in general, and in any case we must introduce complex basis phases to extract dispersion relations.

To motivate our choice of basis phases, first consider a zeroth-order set of one-hole basis states $\{|\mathcal{S}\rangle_0\}$ defined by applying a site-ordered string of fermion operators c_{n,s_z}^\dagger to the vacuum. For example, our initial Néel-and-hole state on the 4×4 lattice, with the hole at site 1, $\mathbf{x}_h = (0, 0)$, is

$$|\mathcal{N}(0, 0)\rangle_0 = c_{2-}^\dagger c_{3+}^\dagger c_{4-}^\dagger c_{5-}^\dagger \dots c_{16+}^\dagger |0\rangle. \quad (10)$$

(Our sites are labeled as in Fig. 1 of Dagotto *et al.*¹³) The phases of this basis are inappropriate for Monte Carlo simulations of the Heisenberg antiferromagnet, since every spin flip has a positive H_I matrix element and hence induces a change in sign of the weight factor. The solution of this problem is well known, and is to introduce a new basis set $\{|\mathcal{S}\rangle_1\}$ with overall phases of $(-1)^{N_{\text{SF}}}$, where N_{SF} is the number of spin flips required to reach the basis state starting from a reference Néel state. In our one-hole problem this specifies the *relative* phases *within each subset* of one-hole basis states $\{|\mathcal{S}, \mathbf{x}_h\rangle\}$ that share the same hole location \mathbf{x}_h . Note, however, that we are still free to specify the overall phase of each of these basis subsets. It is this freedom that allows us to extract the dispersion relation for the hole, since this relative phase is determined by the total momentum of the state.

Momentum eigenstates are defined by their behavior under translations; a translation of a state of momentum \mathbf{k} by \mathbf{a} returns the same state with a \mathbf{k} -dependent phase,

$$T(\mathbf{a}) |\mathbf{k}\rangle = e^{-i\mathbf{k}\cdot\mathbf{a}} |\mathbf{k}\rangle. \quad (11)$$

We use this property of momentum eigenstates to choose our basis phases so that all states with momenta other than a specified \mathbf{k} are projected out in the sum over final hole sites, this sum being implicit in the calculation of the average weight $\langle w \rangle$ in (7). Specifically, we use as our basis states translations of states with the hole at the origin, with a multiplicative phase factor of $\exp\{+i\mathbf{k}\cdot\mathbf{a}\}$. For example, to extract $\mathbf{k} = (0, 0)$ energies, the basis state corresponding to a Néel-and-hole state with the hole at $\mathbf{x}_h = (1, 0)$ is taken to be the pure translated state $T|\mathcal{N}\rangle_0$,

$$\begin{aligned} T(\mathbf{x}_h = \hat{\mathbf{x}}) |\mathcal{N}(0, 0)\rangle_0 &= c_{3-}^\dagger c_{4+}^\dagger c_{1-}^\dagger c_{6-}^\dagger \dots c_{13+}^\dagger |0\rangle \\ &= (-1)c_{1-}^\dagger c_{3-}^\dagger c_{4+}^\dagger c_{5+}^\dagger \dots c_{16-}^\dagger |0\rangle \\ &= (-1)|\mathcal{N}(1, 0)\rangle_0. \end{aligned} \quad (12)$$

Similarly, the $\mathbf{k} = (0, 0)$ Néel-and-hole basis state with hole location (n_x, n_y) is

$$T(n_x \hat{\mathbf{x}} + n_y \hat{\mathbf{y}}) |\mathcal{N}(0, 0)\rangle_0 = (-1)^{n_x} |\mathcal{N}(n_x, n_y)\rangle_0. \quad (13)$$

(The factor of $(-1)^{n_x}$ in (13) is induced by the ordering convention [Eq. (10)] used to define the $\{|\mathcal{N}\rangle_0\}$ basis.) In contrast, to extract general \mathbf{k} states we use basis states with plane-wave phases, so that all states with $\mathbf{K} \neq \mathbf{k}$ are eliminated in the average over final hole locations because $\sum_{\mathbf{x}_h} \exp\{i(\mathbf{k} - \mathbf{K}) \cdot \mathbf{x}_h\}$ vanishes unless $\mathbf{K} = \mathbf{k}$. The required Néel-and-hole basis states with general \mathbf{k} and hole location (n_x, n_y) are

$$\exp(+i\mathbf{k} \cdot \mathbf{x}) T(n_x \hat{\mathbf{x}} + n_y \hat{\mathbf{y}}) |\mathcal{N}(0, 0)\rangle_0$$

$$= \exp[+i(k_x n_x + k_y n_y)] (-1)^{n_x} |\mathcal{N}(n_x, n_y)\rangle_0. \quad (14)$$

Previously we specified the relative phases within each fixed-hole-location subbasis $\{|\mathcal{S}, \mathbf{x}_h\rangle\}$ by the Heisenberg-model $(-1)^{N_{\text{SF}}}$ rule. As we have now specified the relative phases of each of these subbases by (14), the relative phases of all basis states are now determined.

The weight-factor phase [Eq. (9)] equals the phase of the product of $-H_{\text{hop}}$ matrix elements [Eq. (1)] between the basis states [Eq. (14)], where the product runs over all hole hops which the random walk has allowed. (We have chosen our phases so spin flips do not change the phase [Eq. (9)]; only hole hops remain as nontrivial $-H_I$ terms in (9).) Inspection of (10) and (14) shows that fermion operator ordering introduces an additional factor of (-1) in the matrix element of $(-H_I)$ for each hole hop in the $\pm\hat{\mathbf{y}}$ directions. This factor combined with the phase multiplying (14) gives the total weight-factor phase $\exp(i\phi)$ we use in (6) and (8) to determine the hole dispersion relation.

As this definition of phases is somewhat complicated, it may be useful to specify the resulting rule for the weight-factor phase $\exp(i\phi)$ in (6) operationally: (i) spin flips have no effect on the phase; (ii) under a hole hop, the phase of the weight changes by a factor of

$$e^{i\Delta\phi} = (-1)e^{-i\mathbf{k}\cdot\Delta\mathbf{x}_h} (-1)^{\Delta N_{\text{SF}}}. \quad (15)$$

The overall (-1) is the product of the intrinsic (-1) in (13) encountered in translating the “zeroth-order” basis states such as (10) by $\pm\hat{\mathbf{x}}$ times the operator-ordering phase (-1) encountered for hole hops along $\pm\hat{\mathbf{y}}$; their combined effect is a (-1) for every hole hop. The second factor is due to the $\exp(i\mathbf{k}\cdot\mathbf{x}_h)$ present in a momentum eigenstate. The third factor is the Heisenberg minus sign which ensures that spin flips never change the sign of the weight. All these may simply be evaluated as an overall phase factor of

$$e^{i\phi(\mathbf{k})} = (-1)^{N_{\text{hop}}} e^{-i\mathbf{k}\cdot[\mathbf{x}_h(f) - \mathbf{x}_h(i)]} (-1)^{\Delta N_{\text{SF}}}, \quad (16)$$

at the end of each walk (at τ_1 or τ_2); note that the first two phase factors on the right-hand side depend only on the initial and final configurations, not on the path followed. The average weight and resulting energy for each momentum can then be calculated using (6), (8), and (16) for each \mathbf{k} . Note that the energies for all momenta are determined concurrently by evaluating average weights with different end-point factors of $\exp[i\phi(\mathbf{k})]$.

III. RESULTS AND DISCUSSION

In our simulations we studied the spectrum of single-hole states on 4×4 and 6×6 lattices. Lanczos results are known for the 4×4 lattice, which served as a test case. For our initial configuration we used a Néel state with a hole at the origin. First, to confirm that the algorithm gives correct results we generated 4×4 energies for the six independent momenta at small t/J values of

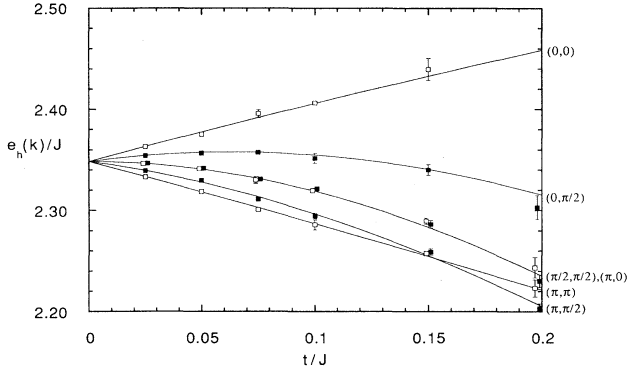


FIG. 1. Lanczos and Monte Carlo results for the $S_{\text{tot}} = 1/2$ one-hole band on the 4×4 lattice.

0.0, 0.025, 0.05, 0.075, and 0.10. For importance sampling we used a simple trial wave function of the form

$$|\psi_0^g(\mathcal{S})\rangle = c e^{-\xi H_0(\mathcal{S})}, \quad (17)$$

and an optimum parameter value of $\xi \approx 0.56$ was found by minimizing the variance of weight-factor moduli. (This is slightly larger than the value used in previous static-hole simulations.²⁰) After some numerical tests we chose to set $\tau_1 = 6.0$, $\tau_2 = 7.0$, and $h_\tau = 0.025/L^2$ (the Euclidean times and h_τ are given in units of J^{-1}), and we generated samples of 2^{22} random walks for each value of t/J . The average weights $\langle w(\tau_1) \rangle$ and $\langle w(\tau_2) \rangle$ are in general complex numbers, but as only the overall time dependence is relevant to the energy we used the modulus of the average weight $|\langle w(\tau) \rangle|$ in (8). The resulting one-hole band is shown together with Lanczos results in Fig. 1 and Table I; evidently, the results are numerically

consistent. [Actually we added (π, π) to all the momenta before displaying the energies in the figures and tables, to change the definition of momentum to that of Refs. 12 and 18, and will use their convention in our subsequent discussion. The weight phases described in the text correspond to the momentum conventions of Refs. 7 and 10.] Our results are also consistent with the known degeneracy of the $(\pi/2, \pi/2)$ and $(\pi, 0)$ multiplets, which is due to a higher symmetry of the 4×4 lattice and is not trivially realized in the Monte Carlo simulation.

Inspection of the weight-factor variance shows that the energy errors increase by about a factor of 3 with each step of $\Delta(t/J) = 0.05$, given these parameters and the simple trial wave function [Eq. (17)]. Since the errors decrease as $1/\sqrt{N_{\text{RW}}}$, to maintain the small statistical errors in Table I we must increase the sample of walks by about a factor of 2^3 for each step of $\Delta(t/J) = 0.05$. This is illustrated by the $t/J = 0.15$ points, which are averages of 2^{25} walks and in consequence have errors comparable to the $t/J = 0.10$ points with $N_{\text{RW}} = 2^{22}$. For the final measurements at $t/J = 0.20$ we again generated 2^{25} walks, and the anticipated increase in error by approximately a factor of 3 relative to $t/J = 0.15$ is evident. For most levels the error is still relatively small, ± 0.005 to ± 0.012 , but for the worst case of $\mathbf{k} = (0, 0)$ we find a large error of about ± 0.05 . We emphasize that the rapid growth of statistical errors with t/J is due to the large Euclidean measurement time τ_1 used in these simulations. This large τ_1 is required to remove excited-state contributions from the very simple trial wave function (17) used in this initial study. Improved Heisenberg-model wave functions with long-range correlations have been described in the literature (see, for example, Sec. III E of the review by Manousakis³⁴ and papers by Liang, Doucot, and Anderson,³⁵ and Dagotto and Schrieffer³⁶),

TABLE I. Lanczos and Monte Carlo results for the lowest-lying $S_{\text{tot}} = 1/2$ one-hole band on the 4×4 lattice; we display $e_h(\mathbf{k})/J = (E_h(\mathbf{k}) - E_0)/J$ at each independent momentum vs t/J .

t/J	0.025	0.050	0.075	0.100	0.150	0.200
$\mathbf{k} = (0, 0)$	2.36331 2.3631(8)	2.37779 2.3754(19)	2.39200 2.3958(40)	2.40593 2.4064(11)	2.43291 2.4397(109)	2.45864 2.5291(531)
$(\pi/2, 0)$	2.35456 2.3543(6)	2.35765 2.3566(18)	2.35780 2.3573(18)	2.35502 2.3517(49)	2.34077 2.3402(54)	2.31538 2.3030(118)
$(\pi, 0)$	2.34670 2.3463(6)	2.34112 2.3412(15)	2.33189 2.3300(34)	2.31911 2.3195(21)	2.28341 2.2895(31)	2.23529 2.2436(100)
$(\pi/2, \pi/2)$	2.34670 2.3468(6)	2.34112 2.3418(6)	2.33189 2.3309(14)	2.31911 2.3214(22)	2.28341 2.2863(36)	2.23529 2.2302(62)
$(\pi, \pi/2)$	2.33970 2.3393(4)	2.32804 2.3296(12)	2.31367 2.3111(15)	2.29670 2.2946(29)	2.25540 2.2590(32)	2.20513 2.2030(49)
(π, π)	2.33355 2.3331(7)	2.31829 2.3187(12)	2.30277 2.3007(21)	2.28700 2.2859(50)	2.25472 2.2576(23)	2.22145 2.2232(85)

and by incorporating such an improved wave function we anticipate that a much shorter evolution in Euclidean time will give comparably accurate results. As these will experience fewer hole hops, and hence smaller rotations of the weight phase, the “minus-sign problem” will be considerably reduced.

Although no numerical results have previously appeared for the t - J model bandwidth on lattices larger than 20 sites, there are theoretical arguments that the one-hole band structure at small t/J should depend strongly on the lattice size.^{8,18,37} Perturbation theory in the hopping parameter^{13,18,37} finds that the small- t/J dispersion relation is

$$e_h(\mathbf{k}, t) = e_h(t=0) + Z_w 2t [\cos(k_x) + \cos(k_y)] + O(t^2/J), \quad (18)$$

where Z_w is a bandwidth renormalization; the small- t/J bandwidth is $W = Z_w 8t$. $Z_w = +1$ for a free fermion on the lattice, and for the hole it is a function of both S_{tot} and L , and involves an overlap of initial and final spin wave functions.³⁷ It has been suggested that this bandwidth renormalization is actually zero in the bulk limit,⁸ although probably only for low-spin states³⁷ ($S_{\text{tot}}/L^2 \rightarrow 0$), because the staggered-magnetized spin background reduces the overlap between one-hop initial and final spin states to zero. This effect has also been attributed to a dimerization of the lattice by the staggered magnetization in the bulk limit,⁸ which reduces the size of the effective Brillouin zone and leads to degeneracies between levels with momenta that differ by (π, π) . This implies $Z_w = 0$, so the bulk-limit bandwidth at leading order in the hopping parameter expansion is $O(t^2/J)$. At large but finite L , simple arguments involving the spin-wave gap (which vanishes $\propto 1/L^2$) and degeneracies expected at the supersymmetric point^{37–39} ($t/J = 1/2$) lead one to expect that Z_w for the low-spin states should approach zero as κ/L^2 .

One-hole band structure at second order in the hopping parameter has been discussed by Dagotto *et al.*,¹³ who obtained a general three-parameter form for the $O(t^2/J)$ one-hole dispersion relation. Their Eq. (20) is equivalent to the form

$$e_h(\mathbf{k}, t)/J = v_1 + v_2 [\cos(k_x) + \cos(k_y)] \left(\frac{t}{J}\right) + \left\{ v_3 [\cos^2(k_x) + \cos^2(k_y)] + v_4 [\cos(k_x) \cos(k_y)] + v_5 \right\} \left(\frac{t}{J}\right)^2. \quad (19)$$

There is a relation between the coefficients $\{v_i\}$ in $O(t^2/J)$ perturbation theory, which is implicit in their definition in terms of the $\{\alpha_i\}$ of Dagotto *et al.*,

$$v_2 = 2Z_w = -2\alpha_0, \quad (20)$$

$$v_3 = -\frac{8(\alpha_1^2 + \alpha_2)}{\alpha}, \quad (21)$$

$$v_4 = -\frac{16\alpha_1(1 + \alpha_2)}{\alpha}, \quad (22)$$

$$v_5 = -\frac{4(1 - \alpha_2)^2}{\alpha}, \quad (23)$$

where

$$\alpha \equiv \frac{3}{2} - \frac{9}{2}\alpha_0 + 2\alpha_1 + \alpha_2. \quad (24)$$

In our fits to numerical results we do not impose the constraint but instead treat all five coefficients $\{v_i\}$ as free parameters.

First, we consider the 4×4 case; the values of the coefficients are found from Lanczos data to be

$$v_1 = 2.3486, \quad (25)$$

$$v_2 = 0.2976, \quad (26)$$

$$v_3 = 0.6950, \quad (27)$$

$$v_4 = 1.390, \quad (28)$$

$$v_5 = -2.990. \quad (29)$$

Note in particular the linear- t bandwidth narrowing relative to the free-fermion value,

$$Z_w(4 \times 4) = v_1/2 = 0.1488, \quad (30)$$

and the exact relation on the 4×4 lattice,

$$2v_3 = v_4, \quad (31)$$

which is a result of the degeneracy between $(\pi, 0)$ and $(\pi/2, \pi/2)$ levels on this lattice, since, to $O(t^2/J)$,

$$e_h(\pi, 0) - e_h(\pi/2, \pi/2) = (2v_3 - v_4) \left(\frac{t^2}{J}\right). \quad (32)$$

To study one-hole band structure on the 6×6 lattice we generated Monte Carlo energies for the ten independent momentum levels using the same parameters and trial wave function as in the 4×4 simulation. We measured energies at $t/J = 0.0, 0.025, 0.050, 0.075$, and 0.10 , with 2^{25} walks at each t/J value. The 6×6 Heisenberg model ground-state energy with the same Monte Carlo parameters was found to be $E_0 = -24.4406 \pm 0.0010$, which is consistent with our previous Monte Carlo result²⁰ and with the recent Lanczos result of Schulz and Ziman,⁴⁰ $E_0 = -24.4394$. In the 6×6 one-hole systems, however, we found somewhat slower convergence of Monte Carlo energies with Euclidean time, and in the static-hole case we estimate the resulting bias due to running at $\tau_1 = 6$ to be $\Delta E \approx +0.023$. We have added this systematic correction to our measured energies, and the resulting final estimates are given *with statistical errors only* in Table II. The uncertainty in this bias is about ± 0.005 , which is somewhat larger than the statistical errors of most of the 6×6 one-hole energies. Thus our errors are dominantly systematic rather than statistical. To provide a

TABLE II. Monte Carlo results for the lowest-lying $S_{\text{tot}} = 1/2$ one-hole band on the 6×6 lattice; we display $e_h(\mathbf{k})/J$ at each independent momentum vs t/J . The quoted errors are statistical only; there is an overall systematic uncertainty of about ± 0.005 (see text for discussion).

t/J	0.025	0.050	0.075	0.100
$\mathbf{k} = (0, 0)$	-23.179(2)	-23.171(4)	-23.162(5)	-23.150(18)
$(\pi/3, 0)$	-23.182(2)	-23.177(3)	-23.179(3)	-23.181(11)
$(2\pi/3, 0)$	-23.186(1)	-23.185(2)	-23.196(3)	-23.212(5)
$(\pi, 0)$	-23.187(1)	-23.186(3)	-23.197(3)	-23.215(8)
$(\pi/3, \pi/3)$	-23.184(2)	-23.184(3)	-23.190(3)	-23.199(7)
$(2\pi/3, \pi/3)$	-23.188(1)	-23.190(3)	-23.203(4)	-23.213(5)
$(\pi, \pi/3)$	-23.188(1)	-23.191(3)	-23.205(3)	-23.216(3)
$(2\pi/3, 2\pi/3)$	-23.190(1)	-23.195(3)	-23.211(4)	-23.222(4)
$(\pi, 2\pi/3)$	-23.190(1)	-23.195(3)	-23.209(4)	-23.221(3)
(π, π)	-23.190(2)	-23.194(3)	-23.210(5)	-23.203(5)

parametrization of the 6×6 band and to extrapolate to larger t/J we carried out a least-squares fit of the 6×6 data to the $O(t^2/J)$ hopping parameter expansion [Eq. (19)]. Our results are presented in Table II and Fig. 2. The 4×4 (Fig. 1) and 6×6 (Fig. 2) bands are plotted on the same scale; comparison of these figures clearly shows evidence for band narrowing on the larger lattice. To avoid confusion in Fig. 2 we show Monte Carlo results only for three representative levels, which in order of increasing energy are $(2\pi/3, 2\pi/3)$, $(\pi/3, \pi/3)$, and $(0, 0)$; the latter generally has the largest statistical errors. We also show the fitted band energies [Eq. (19)] for all levels. The fitted coefficients $\{v_i\}$ are

$$v_1 = -23.185, \quad (33)$$

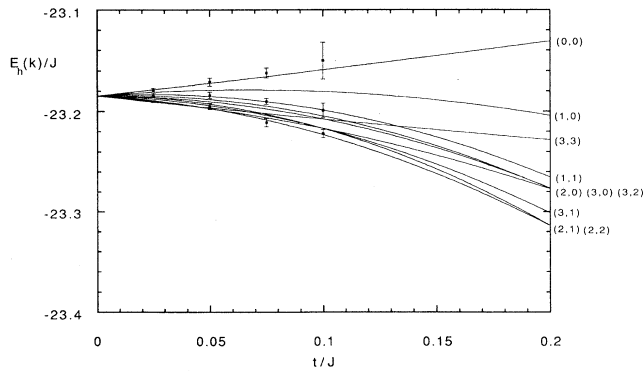


FIG. 2. Monte Carlo results for three 6×6 levels and fitted curves for all levels. (n_x, n_y) denotes momentum $(n_x\pi/3, n_y\pi/3)$; only $(0,0)$, $(1,1)$, and $(2,2)$ data points are displayed.

$$v_2 = 0.122, \quad (34)$$

$$v_3 = 1.23, \quad (35)$$

$$v_4 = 1.21, \quad (36)$$

$$v_5 = -3.54. \quad (37)$$

(We have not subtracted the imprecisely known 6×6 static hole energy E_{0h} from v_1 in this case.) It is difficult to estimate the total error in these coefficients, since $\{E(\mathbf{k})\}$ values determined from a single set of walks are highly correlated. As noted above, the $t/J = 0$ intercept v_1 has a systematic uncertainty of about ± 0.005 . We have attempted to estimate the uncertainty in the remaining coefficients both by modifying the details of the fit and by comparing with the 4×4 case; this suggests that the small- t/J bandwidth coefficients v_2 is uncertain by about ± 0.01 . The second-order coefficients v_3, v_4 , and v_5 are much less well determined because they are weighted by the small quantity $(t/J)^2$; these have estimated uncertainties of $\approx 20\%$.

The linear- t bandwidth coefficient v_2 [Eq. (34)] has evidently decreased to about 0.4 of its value on the 4×4 lattice [Eq. (26)]. In comparison, the arguments that it approaches zero as κ/L^2 lead us to expect a value about $4/9$ as large as the 4×4 coefficient, which is consistent with our Monte Carlo results at present accuracy. The fitted bandwidth renormalization on the 6×6 lattice is

$$Z_w(6 \times 6) = 0.061, \quad (38)$$

and so the linear- t hole bandwidth on the 6×6 lattice with $S_{\text{tot}} = 1/2$ is about a factor of 20 smaller than for

a free fermion with the same hopping parameter. Our numerical results clearly support the conjecture that the linear- t component of the one-hole bandwidth vanishes in the bulk limit.

Assuming that the fitted higher-order coefficients are approximately correct, we see that the effect of increased lattice size is primarily to increase the coefficient v_3 . This lifts the degeneracy of $(\pi, 0)$ and $(\pi/2, \pi/2)$ levels found on the 4×4 lattice, and $(\pi/2, \pi/2)$ becomes the lower level. [Of course the 6×6 lattice has no $(\pi/2, \pi/2)$ state; this conclusion applies to $4n \times 4n$ lattices.]

We find that the hopping-parameter expansion [Eq. (19)] with numerically determined coefficients [Eqs. (25)–(29)] gives a qualitatively correct picture of the 4×4 band to $t/J \sim 0.5$. It may therefore be of interest to present our extrapolated results for the 6×6 band for comparison with future Monte Carlo studies. Our result [Eq. (19)] with fitted coefficients [Eqs. (33)–(37)] is shown in Fig. 3 for the range $0 \leq t/J \leq 0.5$. Since the small- t/J behavior is not evident in this figure, we shall briefly summarize the sequence of ground-state levels. The (π, π) level is the 6×6 ground state for $0.0 < t/J \lesssim 0.04$; near $t/J = 0.04$ the $(2\pi/3, \pi)$ and $(2\pi/3, 2\pi/3)$ levels cross the (π, π) , and $(2\pi/3, \pi)$ may be the lowest level for a short interval near $t/J = 0.04$. The $(2\pi/3, 2\pi/3)$ is the 6×6 ground state for $0.05 \lesssim t/J \lesssim 0.20$, where it crosses $(2\pi/3, \pi/3)$, which presumably remains the ground state until large t/J values are reached and the transition to the Nagaoka state begins. This $(2\pi/3, \pi/3)$ level is expected to be the 6×6 ground state at moderate t/J because it is closest in energy to the $(\pi/2, \pi/2)$ minimum of the $O(t^2/J)$ terms in (19).

As a result of the simple importance sampling (17) used here, we cannot at present resolve band structure at appreciably larger values of t/J , but we anticipate that this will be possible given an improved trial wave function. This has been demonstrated by Boninsegni and Manousakis,²³ who used a trial wave function with long-range correlations in a similar Monte Carlo algorithm and were able to follow the $(\pi/2, \pi/2)$ one-hole level to

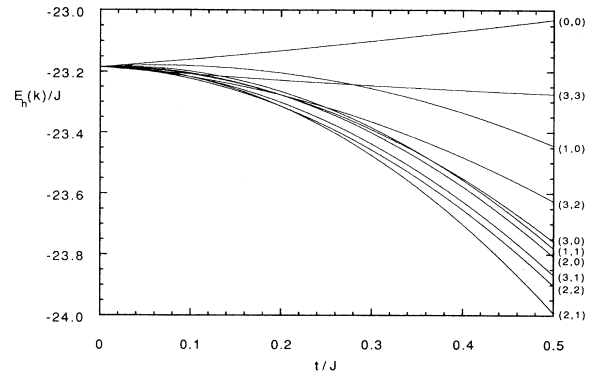


FIG. 3. 6×6 t - J band structure from extrapolated Monte Carlo data (n_x, n_y) denotes momentum $(n_x\pi/3, n_y\pi/3)$.

$t/J = 5$ on large lattices. The advantage of using a more accurate spin-wave function is that convergence to the ground state to a specified accuracy occurs at a smaller Euclidean time, in which fewer hole hops take place. In consequence one may carry out Monte Carlo measurements at appreciably larger values of t/J . In future we plan to extend our Monte Carlo study of band structure in the t - J model to values relevant to the superconductors through the incorporation of similar improved importance sampling.

ACKNOWLEDGMENTS

We would like to thank E. Dagotto, V. Elser, D. Huse, A. E. Jacobs, R. Joynt, S. Liang, E. Manousakis, A. Moreo, E. S. Swanson, and T. A. L. Ziman for useful discussions of various aspects of this work. This research was sponsored by the United States Department of Energy under Contract No. DE-AC05-84OR21400 and Martin Marietta Energy Systems Inc, and by the State of Tennessee Science Alliance Center under Contract No. R01-1062-32.

¹J.E. Hirsch, Phys. Rev. Lett. **54**, 1317 (1985).

²M. Marder, N. Papanicolaou, and G.C. Psaltakis, Phys. Rev. B **41**, 6920 (1990).

³V.J. Emery, S.A. Kivelson, and H.Q. Lin, Phys. Rev. Lett. **64**, 475 (1990).

⁴W.O. Putikka, M.U. Luchini, and T.M. Rice, Phys. Rev. Lett. **68**, 538 (1992).

⁵A. Moreo, D.J. Scalapino, and E. Dagotto, Phys. Rev. B **43**, 11442 (1991).

⁶E. Dagotto, A. Moreo, F. Ortolani, D. Poilblanc, and J. Riera, Phys. Rev. B **45**, 10741 (1992).

⁷Y. Hasegawa and D. Poilblanc, Phys. Rev. B **40**, 9035 (1989).

⁸V. Elser, D.A. Huse, B.I. Shraiman, and E.D. Siggia, Phys. Rev. B **41**, 6715 (1990).

⁹T. Itoh, M. Arai, and T. Fujiwara, Phys. Rev. B **42**, 4834 (1990).

¹⁰J. Bonča, P. Prelovšek, and I. Sega, Phys. Rev. B **39**, 70

(1989).

¹¹J. Riera, Phys. Rev. B **40**, 833 (1989).

¹²E. Dagotto, A. Moreo, and T. Barnes, Phys. Rev. B **40**, 6721 (1989).

¹³E. Dagotto, R. Joynt, A. Moreo, S. Bacci, and E. Gagliano, Phys. Rev. B **41**, 9049 (1990).

¹⁴C.-X. Chen and H.-B. Schüttler, Phys. Rev. B **41**, 8702 (1990).

¹⁵E. Dagotto, J. Riera, and A.P. Young, Phys. Rev. B **42**, 2347 (1990).

¹⁶E. Dagotto, Int. J. Mod. Phys. B **5**, 907 (1991).

¹⁷K. Fabricius, U. Löw, and K.-H. Mütter, Phys. Rev. B **44**, 9981 (1991).

¹⁸T. Barnes, A.E. Jacobs, M.D. Kovarik, and W.G. Macready, Phys. Rev. B **45**, 256 (1992).

¹⁹N. Bulut, D. Hone, D.J. Scalapino, and E.Y. Loh, Phys. Rev. Lett. **62**, 2192 (1989).

²⁰T. Barnes and M.D. Kovarik, Phys. Rev. B **42**, 6159 (1990).

- ²¹E. Manousakis, Phys. Rev. B **45**, 7570 (1992).
- ²²E.Y. Loh, J.E. Gubernatis, R.T. Scalettar, S.R. White, D.J. Scalapino, and R.L. Sugar, Phys. Rev. B **41**, 9301 (1990).
- ²³M. Boninsegni and E. Manousakis, Phys. Rev. B **46**, 560 (1992).
- ²⁴M. Takahashi, Phys. Rev. Lett. **62**, 2313 (1989).
- ²⁵T. Barnes, G.J. Daniell, and D. Storey, Nucl. Phys. B **265** [FS15], 253 (1986).
- ²⁶T. Barnes and G.J. Daniell, Phys. Rev. B **37**, 3637 (1988); see also T. Barnes, in Proceedings of *Computational Atomic and Nuclear Physics at One Gigaflop*, edited by C. Bottcher, M.R. Strayer, and J. McGrory Vol. 16 of *Nuclear Science Research Conference Series* (Harwood Academic, City, 1989), pp. 83–106.
- ²⁷T. Barnes and E.S. Swanson, Phys. Rev. B **37**, 9405 (1988).
- ²⁸T. Barnes and D. Kotchan, Phys. Rev. D **35**, 1947 (1987); D.Kotchan, Ph.D. thesis, University of Toronto, 1990.
- ²⁹G.Gronidin, in *HADRON '91* Proceedings of the IVth International Conference on Hadron Spectroscopy, edited by S. Oneda and D.C. Peaslee (World Scientific, Singapore, 1992), pp. 783–788.
- ³⁰T. Barnes, K.J. Cappon, E. Dagotto, D. Kotchan, and E.S. Swanson, Phys. Rev. B **40**, 8945 (1989).
- ³¹T. Barnes, E. Dagotto, J. Riera, and E.S. Swanson, Phys. Rev. B **47**, 3196 (1993).
- ³²T. Barnes, E. Dagotto, A. Moreo, and E.S. Swanson, Phys. Rev. B **40**, 10997 (1989).
- ³³T. Barnes, Int. J. Mod. Phys. C **2**, 659 (1991).
- ³⁴E. Manousakis, Rev. Mod. Phys. **63**, 1 (1991).
- ³⁵S. Liang, B. Doucot, and P.W. Anderson, Phys. Rev. Lett. **61**, 365 (1988).
- ³⁶E. Dagotto and J.R. Schrieffer, Phys. Rev. B **43**, 8705 (1991).
- ³⁷T. Barnes, in *High-Temperature Superconductivity; Physical Properties, Microscopic Theory, and Mechanisms*, Proceedings of the University of Miami Workshop on Electronic Structure and Mechanisms for High Temperature Superconductivity, edited by J. Ashkenazi, S.E. Barnes, F. Zuo, G.C. Vezzoli, and B.M. Klein (Plenum, New York, 1992), pp. 503–513.
- ³⁸D. Förster, Int. J. Mod. Phys. B **3**, 1783 (1989).
- ³⁹K.J. Cappon, Phys. Rev. B **43**, 8698 (1991).
- ⁴⁰H.J. Schulz and T.A.L. Ziman, Europhys. Lett. **18**, 355 (1992).